WATER RESOURCES RESEARCH, VOL. 46, W03530, doi:10.1029/2009WR007759, 2010

Wind sheltering of a lake by a tree canopy or bluff topography

Corey D. Markfort,[1,2] Angel L. S. Perez,[1,3] James W. Thill,[1,2] Dane A. Jaster,[1] Fernando Porté-Agel,[1,2,3] and Heinz G. Stefan[1,2]

Received 26 January 2009; revised 14 October 2009; accepted 28 October 2009; published 27 March 2010.

[1] A model is developed to quantify the wind sheltering of a lake by a tree canopy or a bluff. The experiment-based model predicts the wind-sheltering coefficient a priori, without calibration, and is useful for one-dimensional (1-D) lake hydrodynamic and water quality modeling. The model is derived from velocity measurements in a boundary layer wind tunnel, by investigating mean velocity profiles and surface shear stress development downwind of two canopies and a bluff. The wind tunnel experiments are validated with field measurements over an ice-covered lake. Both wind tunnel and field experiments show that reduced surface shear stress extends approximately 50 canopy heights downwind from the transition. The reduction in total shear force on the water surface is parameterized by a wind-sheltering coefficient that is related to the reduction of wind-affected lake area. While all measurements are made on solid surfaces, the wind-sheltering coefficient is shown to be applicable to the lake surface. Although several canopy characteristics, such as its height, aerodynamic roughness, and its porosity affect the transition of velocity profiles and surface shear stress onto a lake, a relationship based on canopy height alone provides a sufficiently realistic estimate of the wind-sheltering coefficient. The results compare well with wind-sheltering coefficients estimated by calibration of lake water temperature profile simulations for eight lakes.

Citation: Markfort, C. D., A. L. S. Perez, J. W. Thill, D. A. Jaster, F. Porté-Agel, and H. G. Stefan (2010), Wind sheltering of a lake by a tree canopy or bluff topography, *Water Resour. Res.*, *46*, W03530, doi:10.1029/2009WR007759.

1. Introduction

[2] Wind stress and heat flux are arguably the most important causes of large-scale circulation as well as turbulence in small to medium lakes. They strongly affect water quality and ecological processes, and are therefore included in dynamic lake water quality and ecosystem models. Textbooks on limnology [e.g., *Hutchinson*, 1957], the Encyclopedia of Inland Waters [*Rueda and Vidal*, 2009; *Monismith and MacIntyre*, 2009], and reviews of lake hydrodynamics [e.g., *Fischer et al.*, 1979; *Wüest and Lorke*, 2003], all include information on how wind stress causes mixing in lakes. Wind stress on the lake surface induces lake currents, surface and internal waves, and turbulence, all of which can be determining processes for the vertical mixing, the ecology and the geochemistry of a lake, especially in the surface mixed layer (SML) and the benthic boundary layer. Forced convection induced by wind stress on the water surface, and free thermal convection induced by heat loss from the water to the atmosphere are the main processes that generate SML turbulence, and control the transport of momentum, heat, and mass (e.g., dissolved oxygen, CO_2, CH_4, and water vapor) across the air-water interface and within the SML. Yet despite numerous studies, wind stress, especially on small lake surfaces, is still not well understood or easy to quantify [*Wüest and Lorke*, 2003].

[3] In deterministic models of lake water quality, algorithms for internal mixing, and rates of surface gas transfer and evaporative heat exchange at the air-water interface are linked to wind stress on the lake surface. However, the reduction of wind velocity over a lake (wind sheltering) by a tree canopy or a bluff can rarely be included a priori. Wind sheltering is usually considered a posteriori by applying a "wind-sheltering coefficient" to calibrate simulated against observed lake properties, e.g., temperature profiles.

[4] To understand and simulate the wind-driven processes in a lake, wind velocity and shear stress on the water surface must be resolved for the entire lake surface area. Wind sheltering can significantly reduce the area of wind access, especially on small lakes, as is illustrated in Figure 1 by the reflection of visible light on surface waves in Holland Lake (15 ha surface area). Of the Earth's total number of lakes (and other standing water bodies), 99.9% are small, having areas less than 10 km^2. These lakes account for 54% of the cumulative global lake surface area [*Downing et al.*, 2006]. For the majority of the Earth's lentic surface water bodies, wind sheltering is therefore important.

[5] Specifying wind shear on a small lake downwind of a canopy of trees (forest), crops (agricultural fields), buildings (urban areas), or a bluff is difficult because the atmospheric boundary layer (ABL), over the lake, is undergoing a change as the velocity profile is adjusting from a specific land cover to a relatively smooth water surface. In the transition, wind

[1]Saint Anthony Falls Laboratory, University of Minnesota–Twin Cities, Minneapolis, Minnesota, USA.
[2]Department of Civil Engineering, University of Minnesota–Twin Cities, Minneapolis, Minnesota, USA.
[3]National Center for Earth-Surface Dynamics, University of Minnesota–Twin Cities, Minneapolis, Minnesota, USA.

0043-1397/10/2009WR007759

Figure 1. Aerial image of light reflection by surface waves of a lake. Wind is bowing from the land onto the lake, from the right to the left. The image is the result of the wind sheltering effect of trees on the wavefield on the surface of the lake. A wind-sheltered zone is clearly visible (source is USGS).

speed and wind shear stress on a lake surface are reduced compared with observations at a weather station in flat and open terrain. Airport wind data are commonly available, and it would be useful to know how to adjust the measured wind speeds to account for wind sheltering of a nearby lake.

[6] The objective of this study is to evaluate, by laboratory and field measurements, the along-wind evolution of the surface shear stress as wind blows from a rough and tall canopy (e.g., forest) or a bluff onto a relatively smooth lake surface. Velocity measurements in boundary layer wind tunnel simulations of a canopy to lake transition, as well as field measurements over a lake surface downwind from a tree canopy will be obtained and analyzed to determine the along-wind transect of the surface shear stress on the lake surface. A relationship between normalized surface shear stress and distance from the canopy will be used to determine the extent of wind sheltering for a given canopy. From these results, a model will be developed to predict the wind-sheltering coefficient. The predicted wind-sheltering coefficient will be compared to the wind-sheltering coefficient determined from one-dimensional (1-D) lake hydrodynamic/water quality model simulations for eight lakes.

2. Background

[7] Wind shear stress (drag) on a lake surface is an important boundary condition for lake hydrodynamic and water quality models. Information is currently lacking on the distribution of surface shear stress, especially on smaller lake surfaces where sheltering is important. Since momentum and mechanical energy fluxes across the air-water interface scale as the wind speed squared and cubed, respectively, even small spatial variations in surface wind speed can be expected to produce comparatively large spatial variations in wind-driven currents, turbulence, and resulting mass transport in a lake [e.g., *Melville*, 1996].

[8] Many investigators have confirmed that surface area and fetch are the most important parameters controlling momentum and energy transfer at a lake surface and the resulting epilimnion or SML thickness [*Davies-Colley*, 1988; *Gorham and Boyce*, 1989; *Condie and Webster*, 2001; *Boehrer and Schultze*, 2008]. Mass (e.g., dissolved oxygen, CO_2, CH_4, and water vapor) transfer across the air-water interface is also known to depend strongly on wind speed over a lake [*Wanninkhof et al.*, 1985; *Wanninkhof et al.*, 1990; *Wanninkhof et al.*, 2009], but determining where the reference wind speed should be measured is still subject to assumptions. As a result, gas exchange coefficients for lakes, as a function of wind speed, still have a component of uncertainty.

[9] Wind sheltering of a lake is characterized by atmospheric flows, ranging from the ABL adjustment in response to a surface roughness transition, e.g., from low vegetation on flat terrain, to transition from irregular terrain, e.g., between hills or mountains onto a lake surface. Downwind of a roughness transition, the wind velocity profile can be characterized by two layers. The properties of the upper layer depend only on the surface conditions upwind of the transition, while the lower portion of the profile is affected by the new surface condition. This lower region is termed the internal boundary layer (IBL), which grows deeper downwind from the transition [e.g., *Oke*, 1987; *Stull*, 1988; *Garratt*, 1992]. In the lowest approximately 10% of the IBL, referred to as the equilibrium sublayer, the flow is fully adjusted to the new surface with no influence from the upwind surface.

[10] Still the IBL paradigm may be unsuitable for wind sheltering of lakes because many lakes are found in landscapes characterized by tall plant canopies, e.g., trees, where the flow downwind is more complicated than a simple roughness transition, because it also involves a flow separation or wake and a possible recirculation downwind of the transition [*Cassiani et al.*, 2008; *Flesch and Wilson*, 1999; *Wilson and Flesch*, 1999]. The wake region is characterized by the interaction between a lower layer of relatively low velocity wind (or momentum deficit caused by drag induced by the tree canopy) and a region of higher velocity wind flowing above the canopy. At the trailing edge of the canopy, and over the lake surface, the interaction of these two layers of contrasting velocity produces a blending shear layer and downward flux of momentum (Figure 2). The wake effect is accentuated by increasing canopy density or when a lake is surrounded by elevated terrain (i.e., bluff). In that case, the wind field resembles a backward-facing step (BFS) type of circulation, or coherent rotor-like vortices and wake separation [*Cassiani et al.*, 2008].

[11] The ABL transition between canopies and clearings has been investigated numerically by *Liu et al.* [1996], *Patton et al.* [1998], *Wilson and Flesch* [1999], *Yang et al.* [2006], and *Cassiani et al.* [2008], and experimentally by *Chen et al.* [1995], *Irvine et al.* [1997], and *Detto et al.* [2008] among others. Our attention is focused on lakes in flat terrain where the canopy is the dominant cause of wind sheltering. Although a number of studies have been carried out to characterize the ABL downwind of roughness transitions and canopies, the resulting downwind surface shear

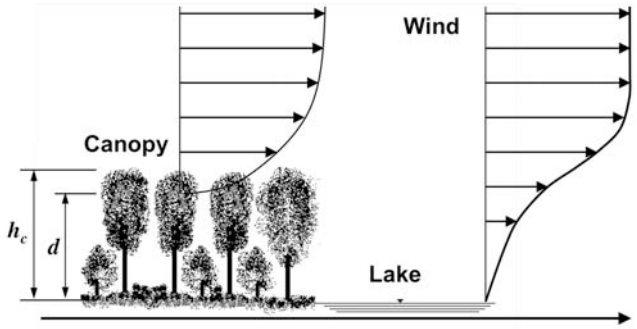

Figure 2. Schematic of wind blowing over a tree canopy at the edge of a lake and the associated windfield transition in the atmospheric boundary layer downwind over the lake. (Also appropriate for flow over a bluff to lake transition.) Here h_c, canopy height; d, displacement height.

stress development continues to resist complete theoretical treatment because all the terms in the time-averaged mean momentum balance remain significant.

[12] For lake modeling, wind speeds measured at local weather stations, e.g., at an airport several kilometers from a lake, are commonly used. The lack of on-lake wind observations as well as the wind sheltering by canopies and bluffs necessitate that 1-D numerical lake hydrodynamic/water quality models are calibrated for wind speed by a wind-sheltering coefficient W_{str} [*Ford and Stefan*, 1980; *Hondzo and Stefan*, 1993]. The wind-sheltering coefficient minimizes the mean residual between simulated model results and observed lake water quality or circulation data (e.g., temperature profiles). This remains the only method for determining the value of W_{str}.

3. Momentum Transfer at a Lake Surface

[13] The transport of momentum across the air-water interface of a lake generally occurs from the atmosphere to the water, whereas heat or mass (e.g., dissolved oxygen, CO_2 CH_4, and water vapor) transfer can occur in either direction. As the wind blows over the water surface, the water surface generates a drag on the wind, slowing the wind nearest the surface. Practical estimates of the shear stress on a lake surface can be obtained from

$$\tau = C_D \rho_a U_z^2, \tag{1}$$

where C_D is a drag coefficient, ρ_a is the density of air, and U_z is the time-averaged wind velocity at some specified height z above the water surface. The wind velocity profile for a fully developed wind field follows the log law on the basis of the von Kármán mixing length similarity theory given by

$$U = \frac{U_*}{\kappa} \ln\left(\frac{z}{z_0}\right), \tag{2}$$

where the von Kármán constant $\kappa = 0.4$, U_* is the shear (friction) velocity defined as $U_* = \sqrt{\tau/\rho_a}$, z is the height, and z_0 is the aerodynamic surface roughness. This similarity form of the velocity profile is only appropriate for neutral atmospheric conditions, and may be adjusted for the effects of buoyancy and density stratification using the Businger-Dyer relationships [cf., *Stull*, 1988; *Garratt*, 1992].

[14] The empirical dimensionless drag coefficient C_D is a function of wave roughness, which is a rather complicated function of both wind speed and the state of wave development or wave age [*Vickers and Mahrt*, 1997; *Wüest and Lorke*, 2003]. The wave age is simply the ratio of wave phase speed to either the wind velocity or roughly 30 times the shear (friction) velocity. By this association of C_D with wave age and mean velocity, a relationship between C_D and U_{10} (mean wind speed measured at 10 m height) is established (Figure 3). For the surface of a lake, the drag coefficient is given by a variation of Charnock's law [*Charnock*, 1955; *Wüest and Lorke*, 2003]:

$$C_{D,10} = \left[\kappa^{-1} \ln\left(\frac{10g}{C_{D,10} U_{10}^2}\right) + 11.3\right]^{-2}, \tag{3}$$

where g is the gravitational acceleration, and U_{10} and $C_{D,10}$ are the mean velocity and surface drag coefficient, respectively, taken at a height of 10 m. Equation (3) is implicit in $C_{D,10}$, but converges within a few iterations, and has been shown to be valid for wind speeds greater than about 5 m s^{-1}.

[15] For small lakes, wind speed is generally low (commonly $U_{10} < 5$ m s^{-1}) because of wind sheltering, giving the greatest variability to the drag coefficient. Because of sheltering and limited fetch, wavefields on lakes are often immature. In addition to spatial wind speed variability, these interactions are the primary complications in determining momentum transfer from the atmosphere into the lake surface boundary layer. For lesser wind speeds, i.e., $U_{10} < 4$ m s^{-1}, the values of observed drag coefficients are yet to be adequately described by any physical model. *Wüest and Lorke* [2003] suggest the following empirical relationship for a wind speed measured at a height of 10 m:

$$C_{D,10} = 0.0044 U_{10}^{-1.15}. \tag{4}$$

Using equations (1)–(4), the wind shear stress can be determined on a water surface. It should be noted that Charnock's law assumes a well-developed wavefield with a wave phase speed similar to the mean wind speed. For less developed wavefields, the frequency of wave formation and destruction

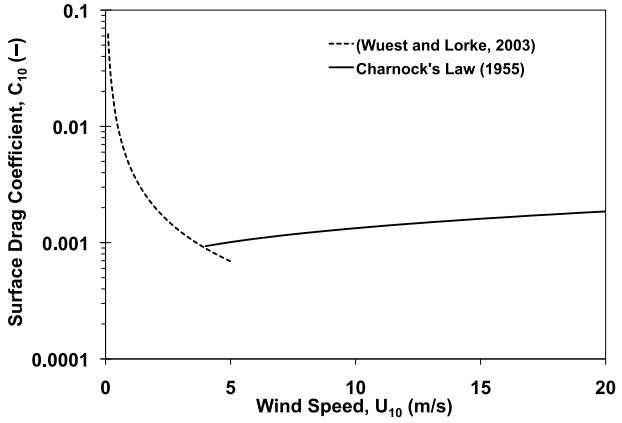

Figure 3. Wind-drag coefficient C_D on a water surface as a function of wind speed U_{10} measured at standard 10 m height above the water surface (equations (3) and (4)).

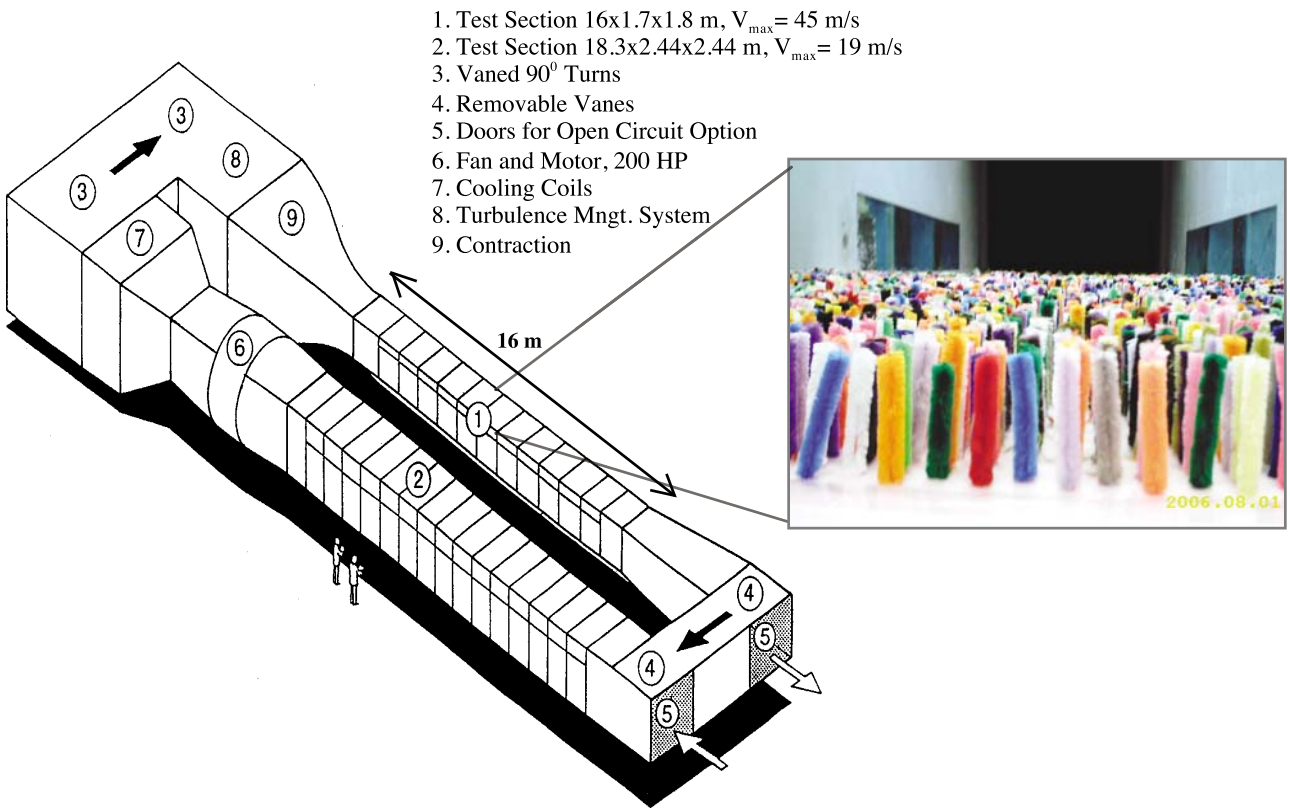

Figure 4. St. Anthony Falls Laboratory Boundary Layer Wind Tunnel (schematic). The inset photograph shows wind tunnel main test section (1) (view upwind) with canopy made of flexible tufted wire (canopy height h_c = 7.5 cm, canopy width is 1.8 m, and canopy porosity is 78%).

is much greater, and requires a larger input of momentum for a given wind speed, resulting in a higher drag coefficient than is predicted. Therefore, the values of shear stress plotted in Figure 3 should be taken as the lower bound on the expected shear stress that would be observed on the lake water surface.

4. Methods of Experimental Investigation

[16] Experiments designed to investigate the development of the wind field and surface shear stress over a lake, downwind from a canopy and a bluff were conducted both in the Boundary Layer Wind Tunnel at the University of Minnesota's Saint Anthony Falls Laboratory (SAFL) and over the ice-covered Round Lake near Andover, Minnesota (latitude, 45°14′24″N; longitude, 93°21′22″W).

4.1. Wind Tunnel Experiments

[17] Three wind tunnel experiments were conducted, to study the evolution of the mean velocity and surface shear stress downwind of the transition from a vegetation canopy (i.e., trees) and a bluff to a lake surface, for two porous canopies and a solid BFS. The experiments were conducted in the main test section of the SAFL wind tunnel, which is 1.7 m wide, 1.8 m high, and approximately 16 m long (Figure 4). In this study, the tunnel was operated in closed circuit and the average free-stream wind velocity was between 10 and 15 m s^{-1}. The experiments were run for neutral conditions at air temperatures between 27°C and 28°C. The turbulent boundary layer was developed with assistance from a tripping mechanism (8 cm picket fence) located at the exit of the wind tunnel contraction, where the test section begins ensuring a deep turbulent boundary layer formed before flow adjusted to the canopy or step. Additional details of the wind tunnel characteristics are provided by *Farell and Iyengar* [1999] and *Carper and Porté-Agel* [2008].

[18] The first experimental setup was considered to be an approximate representation of a canopy of sparse trees or other thin vegetation that ends at the shore of a lake. In this experiment, several layers of wire mesh placed over the wind tunnel floor simulated the canopy. The floor of the wind tunnel by contrast is a smooth surface. The porosity of the wire mesh was 98.0%. The model canopy had a height of 5 cm, covered the total width of the wind tunnel, and extended over a length of $48h_c$ (where h_c is the canopy height) in the flow direction. The wire mesh represents a porous canopy step that ends at $x = 0$.

[19] The Reynolds number, on the basis of canopy (or step) height, is given by

$$\mathrm{Re} = \frac{U_r h_c}{\nu}, \tag{5}$$

where U_r and ν are the reference velocity (measured at the downwind edge of the canopy, $x = 0$, and at six canopy heights, $z = 6h_c$) and kinematic viscosity of air, respectively, and was 4×10^4. The reference velocity is nearly the free-stream velocity and is used solely for comparison of different canopies.

Table 1. Summary of Variables for the Three Wind Tunnel Experiments

	Canopy Material		
	Wire Mesh	Tufted Wire	Solid Step
Canopy Characteristics			
Canopy porosity (%)	98	78	0
Height of canopy h_c (cm)	5	7.5	5.1
Displacement height in canopy d (cm)	2.3	6.6	5.1
Relative displacement height d/h_c	0.46	0.88	1
Roughness of canopy z_{0c} (mm)	13	5	0.04
Roughness of downwind smooth surface z_{0s} (mm)	0.01	0.01	0.01
Velocities and Shear Stresses			
Reference wind velocity U_r[a] (m/s)	13.09	9.46	8.95
Canopy shear velocity U_{*c} (m/s)	1.73	1.00	0.48
Shear stress at canopy top τ_c (N/m^2)	3.86	1.29	0.30
Canopy (step) height Reynolds number (equation (5))	4×10^4	5×10^4	3×10^4

[a] U_r is the velocity measured at the end of the canopy ($x = 0$) at a height $z = 6h_c$ above the wind tunnel floor (h_c is height of the canopy).

[20] Measurements of the time-averaged wind velocity at different positions in the boundary layer were made with a Pitot tube connected to a precision differential manometer (10 torr Baratron differential pressure transducer). The manometer has an accuracy of ±0.0005 mmHg and has a self-calibration option. The outer diameter of the Pitot tube was 3 mm, and it was mounted on a traversing system designed to allow precise vertical positioning above the wind tunnel floor at the centerline of the test section. The Pitot tube does not require calibration, and the accepted lower operation limit is a pressure difference corresponding to a velocity of 0.4–0.5 m/s. Vertical profiles of wind velocity were measured over the wire mesh near the transition ($x = 0$) and also at seven positions downwind of the transition (x/h_c = 4.0, 8.0, 12.0, 22.0, 36.0, 55.2, and 108).

[21] The second experiment represented a homogeneous stand of trees. The model canopy was created from flexible tufted wire (i.e., pipe cleaners). The tufted wires were inserted into a 2.5 cm thick foam board, which was placed on the wind tunnel floor (Figure 4). The canopy had a height of 7.5 cm and porosity of 78%. It covered the total width of the wind tunnel and extended over a length of $53h_c$ in the flow direction. Foam board, of the same thickness but without a canopy, was installed on the wind tunnel floor downwind from the canopy and represented a relatively smooth surface.

[22] The Reynolds number, on the basis of canopy height, was 5×10^4. Wind velocity profiles were measured with the Pitot tube, as in the first experiment, at the edge of the canopy ($x = 0$) and at nine positions downwind of the canopy (x/h_c = 2.7, 5.3, 8.0, 14.7, 26.7, 43.3, 54.3, 79.2, and 89.1).

[23] The third experiment considered flow over a solid BFS representing a bluff or rows of buildings on the upwind side of a lake. The step was created from styrofoam boards and had a height of approximately 5.0 cm. It covered the total width of the wind tunnel and extended over a length of $80h_c$ in the flow direction with an upstream smooth ramp to direct the flow and minimize separation. The wind tunnel floor downwind from the BFS was similarly covered with styrofoam having the same smooth surface roughness. The Reynolds number, on the basis of step height, was 3×10^4. Wind velocity profiles were measured at the end of the canopy ($x = 0$) and at nine positions downwind (x/h_c = 4.0, 8.0, 12.0, 22.0, 40.0, 55.2, 81.4, 118.8, and 133.6).

[24] The roughness of the wind tunnel floor was determined from the measured velocity profiles. To characterize the upwind surface, a velocity profile was measured at the end of the canopy or BFS ($x = 0$) and within the quasi fully developed surface layer above the canopies. Characteristics for all three experiments are summarized in Table 1. The blocking ratio of the canopy on the flow in the wind tunnel test sections was less than 4%, and the ceiling of the wind tunnel was inclined to minimize any longitudinal pressure gradient, which prevented acceleration of the mean flow over the canopy. Further details of the experiments are given in reports by *Jaster et al.* [2007] and *Perez et al.* [2007].

[25] The surface shear stress was calculated for each velocity profile from equation (2), and is a function of the position relative to the windward shoreline. After significant distance downwind of the canopy, shear stress increased asymptotically to a constant value. The calculated shear stress was therefore normalized to the farthest downwind value.

4.2. Field Study

[26] An investigation of the ABL transition from land to a lake at field scale was conducted at Round Lake. Round Lake, as its name implies, is circular with a diameter of approximately 1 km. It is set in a landscape having very flat topography with trees along much of the shoreline. The upwind surrounding area topographically varies by not more than 3 m within approximately 2 km from the lake perimeter (Figure 5). This provides nearly an ideal case to isolate and study the affects of flow over a canopy transition to a small lake.

[27] Vertical wind velocity profiles were measured over the lake in the winter in order to take advantage of the solid ice surface on the lake, which was approximately flat and level. It also made the measurements independent of lake water level, although the roughness of the ice and snow cover is somewhat different from that of the water surface. The data presented here were collected in February and March of 2004.

[28] The objective of the field experiment was to obtain vertical profiles of wind speed at various locations over the lake surface to determine how wind profiles vary downwind of the canopy edge. Three measurement stations were established on the lake surface with a vertical array of wind speed sensors. Station 1 was installed near the center of the lake as a reference. Station 2 was installed in different fixed locations on different days, except on 28 February 2004 when station 2 was used in two locations, denoted as 2a and 2b. Station 3 was mounted on a sled that was periodically moved to different locations on the lake. The different positions were denoted as *M*1, *M*2, *M*3, etc, with the prefix, "*M*" denoting that the station was "mobile" (Figure 5).

[29] At each station, three Met One model 014-A cup anemometers were mounted at various heights on each of the 2.5 m high vertical masts. The heights of the anemometers above the top of the ice/snow cover during each period of measurement are listed in Table 2. In general, the lowest sensor was mounted at a height of 0.3–0.6 m, the middle sensor at a height of 0.8–1.5 m, and the highest sensor at a height of 2.3–2.5 m. A Wind Sentry wind direction sensor (manufactured

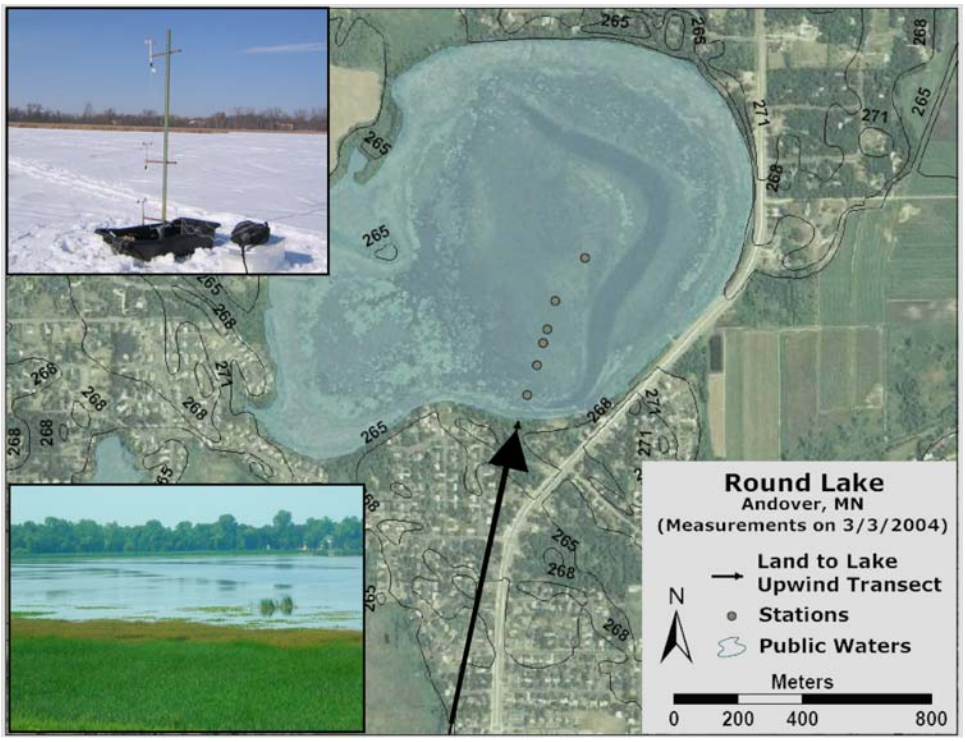

Figure 5. Aerial photograph of Round Lake and surrounding area in 2006. Topographic elevations range from 265 to 268 m above mean sea level. Primary wind direction and measurement stations for experiment on 3 March 2004 are identified. Top inset photo shows view of mobile station on 3 March 2004, and bottom inset photo shows view of the south shore and canopy structure in July 2008.

by R. M. Young) was attached to two of the masts at a height of 1.7 to 1.85 m. In all cases, the wind speed and direction were measured at 10 s intervals.

[30] The wind speed data measured with the cup anemometers were processed using a 12 min moving-window average. The 12 min average wind speeds were plotted as a function of ln(z) to obtain a linear plot, the slope and intercept of which are related to the shear (friction) velocity and the aerodynamic roughness length, respectively, using equation (2). This relationship is only appropriate for near neutral conditions, and the low measurement heights imply that the stability correction should be small in this case. To evaluate the appropriateness of the linearized log law fit to the wind speed profile data, a linear correlation coefficient R^2 was computed at every 12 min interval.

[31] Ultimately, the wind shear stress is a function of fetch, that is, the distance the wind has blown over the water surface from the canopy edge. The fetch was determined from GPS coordinates of each measurement station plotted on a georeferenced map of the lake, and was measured from the tree line to each station in 30° increments around the lake perimeter. Therefore, as the wind direction changed, the fetch changed as a function of direction. Further details of the field experiments are reported by *Thill* [2009].

5. Results and Discussion

5.1. Wind Tunnel Results

[32] Examples of plots of the velocity profiles measured in the wind tunnel downwind from the canopy are shown in Figure 6. The profiles have been normalized in the vertical direction by canopy height h_c and by the reference velocity U_r (measured at $x = 0$ and $z = 6h_c$). The reference velocity represents the free stream velocity, minimizing the effect of the canopy or the wind tunnel ceiling.

5.2. Aerodynamic Characterization of the Wind Tunnel Floor Without a Canopy

[33] The shear (friction) velocity is obtained from the slope of the straight line fit to the data on a semilogarithmic plot and z_0 by extrapolating the straight line to the height $z = z_0$, where $U = 0$ (Figure 7). The wind velocity profile without a canopy is a fully developed turbulent velocity

Table 2. Instrument Heights in the Field Experiments on Round Lake[a]

Instrument	28 February 2004	3 March 2004
	Station 1	
014A-1	0.54	0.35
014A-2	1.10	0.77
014A-3	2.30	2.41
Vane	1.80	1.82
	Station 2	
014A-1	0.43	0.32
014A-2	1.22	1.51
014A-3	2.30	2.45
Vane	1.70	–
	Mobile Station	
014A-1	0.43	0.59
014A-2	1.14	1.24
014A-3	2.32	2.49
Vane	–	1.85

[a]Instruments are anemometer and wind vane. Height is in meters.

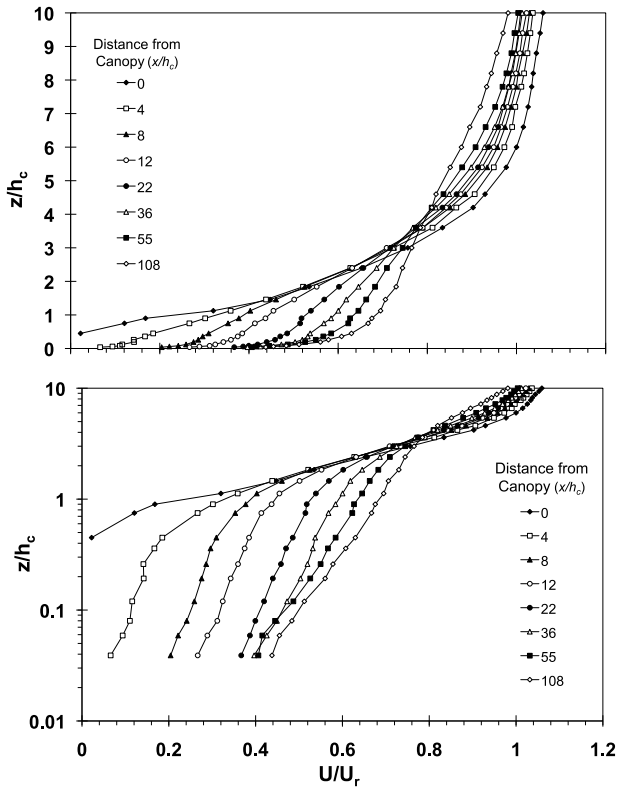

Figure 6. Normalized velocity profiles measured in the wind tunnel downwind from the wire mesh canopy, plotted on (top) arithmetic scale and (bottom) semi-log scale. Vertical distances are from wind tunnel floor and normalized to canopy height (h_c = 5.0 cm). Horizontal velocities U are normalized to reference velocity U_r measured at the edge of the canopy (x = 0) and at six canopy heights above the wind tunnel floor ($z = 6h_c$).

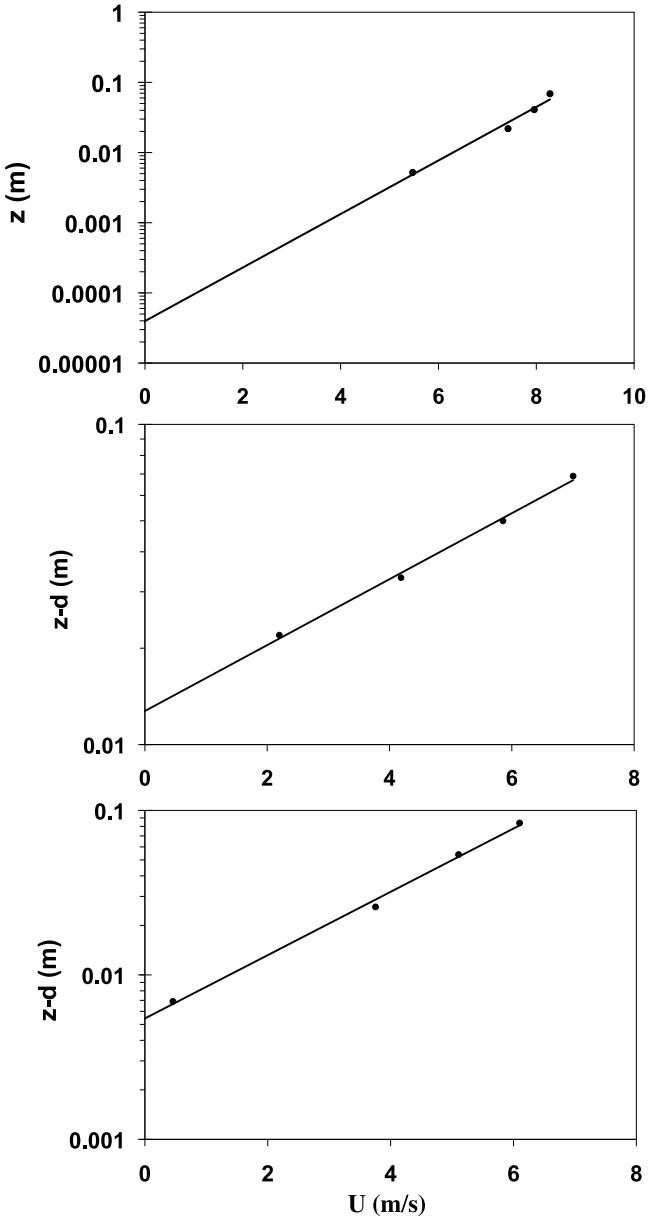

Figure 7. Determination of canopy roughness z_o based on the method given by *Stull* [1988] for the (top) foam board, (middle) wire mesh canopy, and (bottom) tufted wire canopy.

profile as shown by the linearity of the semilogarithmic plot. The data in this plot can be fit to equation (2). From these data, the absolute roughness of the wind tunnel floor was determined to be approximately 1×10^{-5} m (0.01 mm). This value of z_0 is consistent with previous data collected in the same wind tunnel [*Carper and Porté-Agel*, 2008; *Chamorro and Porté-Agel*, 2009]. In our experiments, the wind tunnel floor represents the water surface of the lake, which will have a different roughness, but the relative roughness between the canopy and downwind surface is within a comparable order of magnitude. To illustrate this, we compare our wind tunnel experiments to previously reported values of surface roughness provided for a range of land covers (Table 3). The relative roughness for the tufted wire canopy experiment (0.005 / 0.00001 = 500) is comparable to values from Table 3 for a transition from trees to ice (0.4 / 0.0008 = 500).

5.3. Aerodynamic Characterization of the Experimental Canopies

[34] The aerodynamic characterization of the canopy is essential information to understand how the model canopies compare with the field scale. Because the top of the canopy is not a solid wall, the wind penetrates some distance into the canopy. A description of this process is given by

Table 3. Common Aerodynamic Roughness, Canopy Height, and Zero-Plane Displacement for Different Surfaces[a]

Surface	z_0 (m)	h_c (m)	d/h_c
Open water	$10 \times 10^{-5} - 0.1$	–	–
Ice	1×10^{-3}	–	–
Snow	$10 \times 10^{-4} - 0.5$	–	–
Bare soil	0.001–0.01	–	–
Turf grass	0.0012–0.023	0.015–0.1	–
Prairie grass	0.04–0.20	0.25–1.0	–
Agricultural fields	0.005–0.12	0.18–1.4	–
Woodland trees	0.4–0.9	8–15	0.6–0.75
Coniferous forest	0.28–3.9	10–27	0.61–0.92
Tropical forest	2.2–4.8	32–35	0.85

[a]Here z_0, aerodynamic roughness; h_c, canopy height; d, displacement. Adapted from Table 2.2 of *Oke* [1987] and Table A6 of *Garratt* [1992].

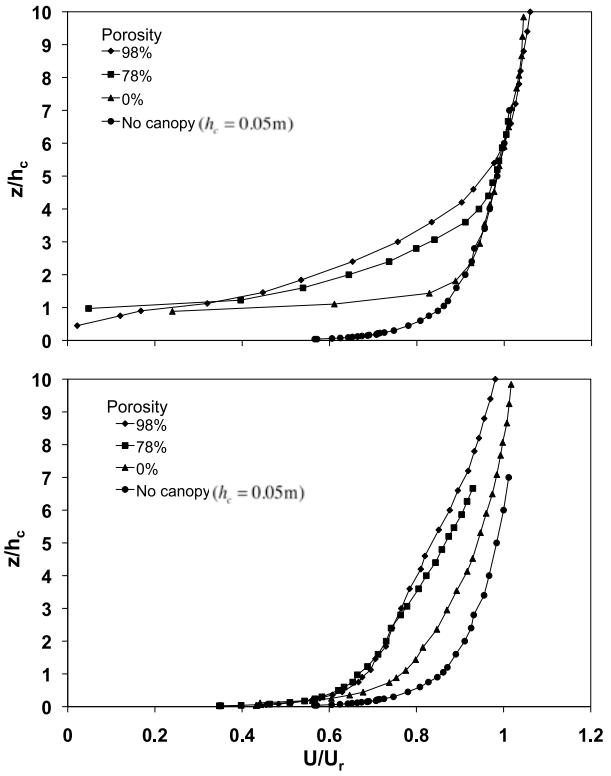

Figure 8. Normalized wind velocity profiles in the wind tunnel for three canopies (0%, 78%, and 98% porosity) at the end of the canopy (top) at $x = 0$ and (bottom) at $x = 90h_c$ downwind from the end of the canopy. A reference velocity profile for without a canopy is plotted and normalized with the height of the solid backward-facing step.

Finnigan [2000], *Stull* [1988], and *Garratt* [1992]. The turbulent velocity profile above a canopy can be fit to the modified log-law equation:

$$U = \frac{U_{*_c}}{\kappa} \ln\left(\frac{z-d}{z_{0c}}\right), \tag{6}$$

where the subscript c defines variables associated with the canopy. Equation (6) is equivalent to equation (2) with the inclusion of displacement height d. The three aerodynamic parameters (U_{*c}, z_{0c}, and d) were estimated by imposing a semilogarithm plot of a velocity profile measured over the canopy. Velocity profiles measured at the edge ($x = 0$) of the canopy (Figure 7) were used to determine all three parameters. The displacement height d for the canopies was determined using an iterative process outlined by *Stull* [1988].

[35] The relative displacement height for the wire mesh, $d/h_c = 0.46$ indicates a penetration to more than half the canopy height, for the tufted wire ("pipe cleaner") canopy, $d/h_c = 0.88$ indicates penetration to 12% of the canopy height, and for a solid backward facing step, $d/h_c = 1$ indicates no penetration. As an estimate, $d = 2/3h_c$, is often used for real vegetation canopies consisting of trees or other plants when direct measurement is not feasible [*Oke*, 1987].

[36] Once the displacement height was determined, the canopy roughness could be obtained by extrapolation of the linear-fitted plot of U versus $\ln(z - d)$ to a zero velocity (Figure 7). The canopy roughness was determined to be approximately 0.013 m for the wire mesh 0.005 m for the "pipe cleaner," and 0.00004 m for the solid step. The canopy shear (friction) velocity, at $x = 0$, was computed using equation (6); it is proportional to the slope of the line shown in Figure 7. Results from the analysis of the canopy data for the three experiments are summarized in Table 1. There was a wide variation in roughness between the three canopies in the wind tunnel. The wire mesh canopy was over 1000 times rougher than the wind tunnel floor, while the pipe cleaner canopy was 500 times rougher, and the solid step was of the same roughness as the wind tunnel floor.

5.4. Structure of the Wind Velocity Field in the Transition From Canopy to Smooth Surface

[37] A separated flow region was detected downstream of the pipe cleaner canopy and the BFS, but not behind the wire mesh canopy. The distance to reattachment was about six to eight times the displacement height of the canopy. This is consistent with results for a BFS given by *Jovic and Driver* [1994], *Le et al.* [1997], *Aider et al.* [2007], and for canopies [*Cassiani et al.*, 2008]. After a distance $x/h_c = 25$, development of the new IBL was identified. It was characterized by rising shear stresses with distance from the canopy. Between $x/h_c = 8$ and $x/h_c = 25$, shear stress on the lake surface is increasing, depending on canopy roughness and porosity.

[38] Three distinct layers were identified in the measured velocity profiles downwind from the point of reattachment: (1) The IBL in response to the shear on the wind tunnel floor; (2) an outer layer far above the canopy; and (3) a mixing/blending layer between layers (1) and (2). With sufficient distance downwind from the canopy, the mixing layer disappears and a single boundary layer with a log law velocity profile forms. These results match the description provided by *Walker and Nickling* [2003] for flow behind dunes and simulated results by *Cassiani et al.* [2008].

5.5. Velocity Deficit and Surface Shear Stress Deficit

[39] The velocity profiles above and downwind from the canopy are affected by the physical characteristics of the canopy such as the shape of the canopy elements and the porosity of the canopy. In particular, the aerodynamic roughness and the displacement height, which characterize the velocity profile above the canopy, are affected.

[40] All wind velocity profiles over the model lake surface show a velocity deficit relative to the wind velocity profile without a canopy (Figure 8), and the roughest canopy has a much larger velocity deficit than the smoothest canopy. A direct comparison of velocity profiles at the end of the canopy ($x = 0$) and downwind ($x/h_c = 90$) illustrates that even at a relatively large distance, there is still a measurable velocity deficit for both of the canopies. Far downwind from the solid backward-facing step ($x/h_c = 90$), the velocity profile had transitioned closer to that of the reference profile without a canopy. It is clear that the behavior of the velocity profile for the BFS is distinctly different from those for the two porous and rough canopies that require a distance longer than $x/h_c = 100$ to overcome the canopy effect entirely.

[41] The results of the wind tunnel experiments indicate that downwind of the canopy, in the transition from the land to the lake surface, the shear velocity (stress) is greatly

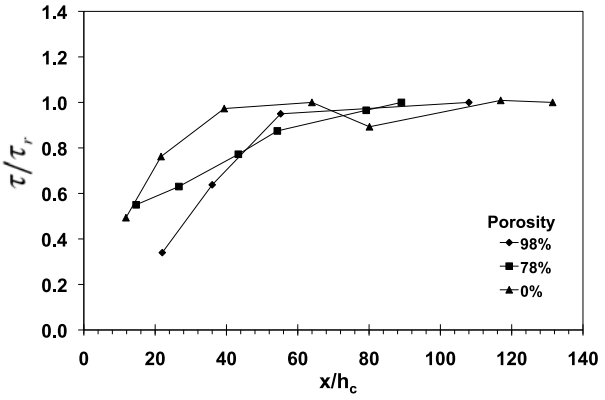

Figure 9. Normalized and time-averaged shear stress τ/τ_r as a function of normalized distance (x/h_c) downwind of three canopies in the wind tunnel.

reduced. When normalized with reference shear (friction) velocity U_{*r}, far downwind, the sheltering extends over a downwind distance of approximately 40 to 60 times the canopy height (Figure 9). Specifically, the experiments show that the shear stress on the surface downwind from the canopy was unaffected by wind sheltering after $x/h_c = 100$, and the effect was less than 10% after $x/h_c = 60$ for all cases. This compares with the theoretical form that surface shear stress is related to sheltering element height by $\tau \sim (h/x)$, developed by *Counihan et al.* [1974] for an array of roughness elements and verified by *Bradley and Mulhearn* [1983]. Similar to the result found in the field by *Bradley and Mulhearn* [1983], our results for surface shear stress were found to adjust at a slower rate than given by the model of *Counihan et al.* [1974].

[42] These results lead to the conclusion that surface shear stresses recover from the wind sheltering effect much faster than velocity profiles downstream from the canopy. This agrees with previous results for roughness transitions [*Bradley*, 1968; *Chamorro and Porté-Agel*, 2009].

5.6. Field Study Results

[43] The results from the field study of shear (friction) velocity, calculated as discussed in the previous section, are summarized in Figure 10, showing station locations relative to the upwind shoreline. Since the mean wind speed was not constant during the field experiments, shear (friction) velocities had to be normalized to account for the nonstationary wind field. All measurements were referenced to a

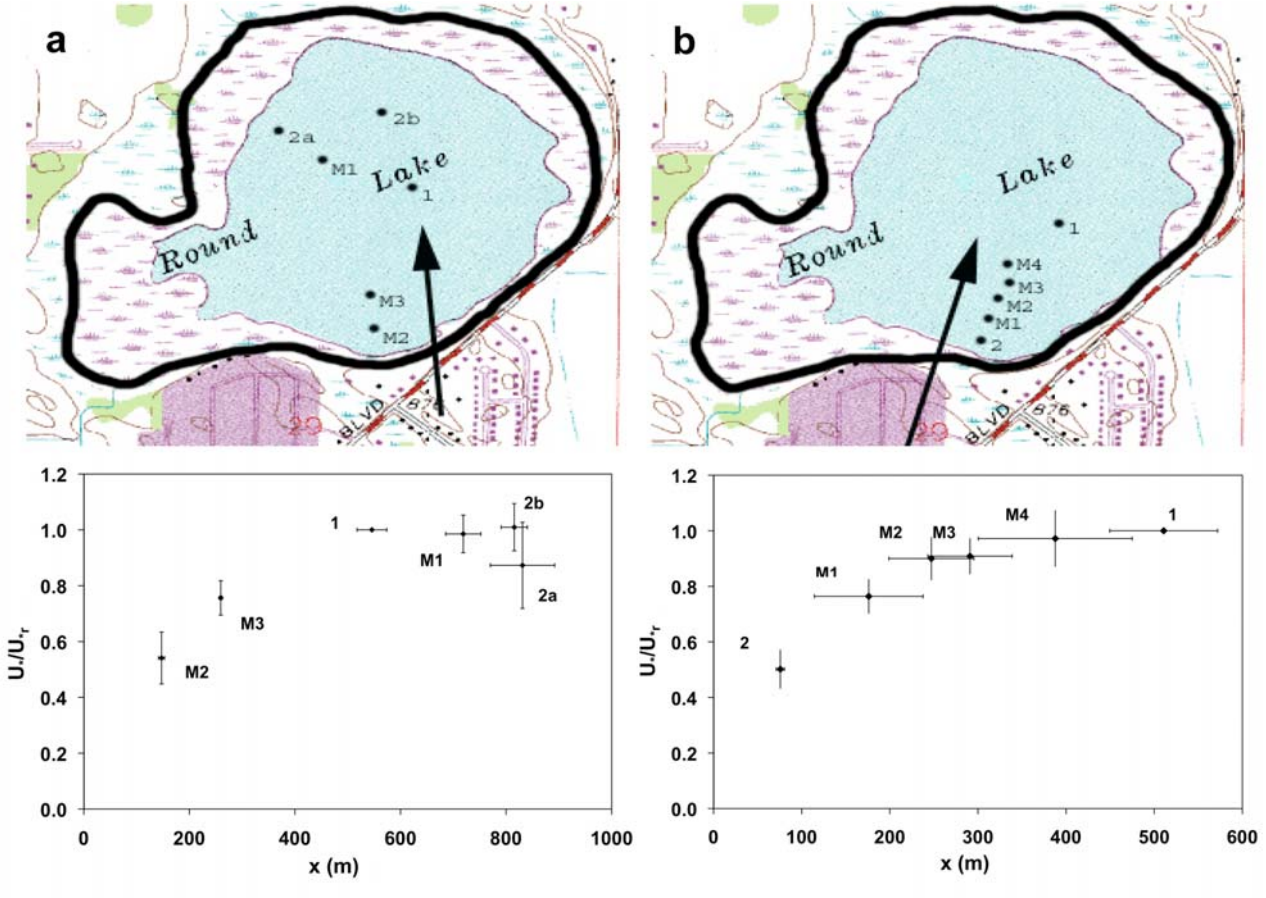

Figure 10. Measurement station locations for wind speed measurements on (a) 28 February 2004 and (b) 3 March 2004, where "*M*" identifies mobile stations and the arrow indicates mean wind direction during the measurement period. The bottom plots show normalized and time-averaged shear velocity U_*/U_{*r} as a function of distance from the tree line. Error bars indicate one standard deviation of measurements.

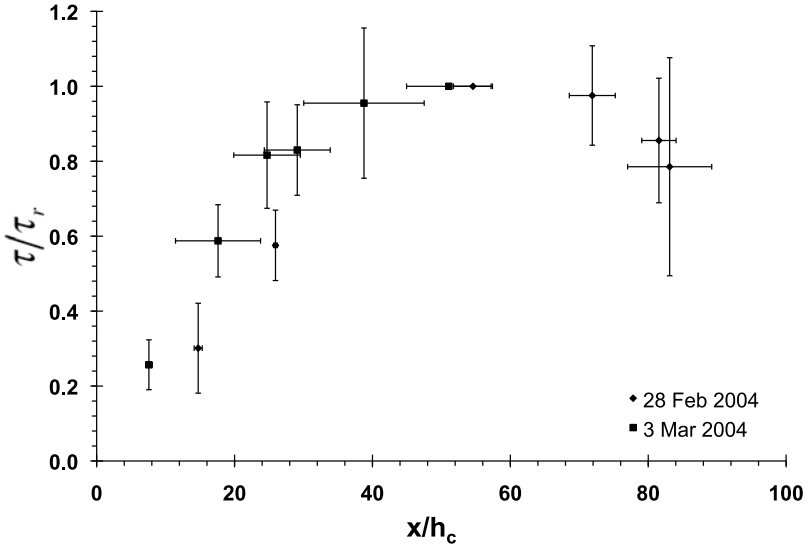

Figure 11. Normalized and time-averaged shear stress τ/τ_r as a function of normalized distance x/h_c from shoreline trees at Round Lake, Andover, MN.

time-variable baseline velocity to make meaningful comparisons. This was accomplished by dividing each value of U_* by the corresponding value of U_* measured at station 1. These normalized values of U_* from each station were averaged for the entire duration of the measurement. The variation in normalized U_* throughout the sampling period is indicated by error bars, which represent one standard deviation about the mean. Sampling periods ranged from a minimum of just over an hour, for the mobile stations, to about 5 h for the fixed stations.

[44] The surface shear stress or shear (friction) velocity on a lake surface is a function of distance from the canopy. Therefore, normalized shear (friction) velocities were plotted against distance. Like the shear (friction) velocity data, the multiple fetch values are averaged over the total sampling period for each station, and represented as a single point with error bars indicating one standard deviation about the mean.

[45] The aerodynamic roughness on the lake ice/snow cover was determined to be in the range from 0.0005 to 0.004 m for the various station locations. The measurements confirm that the aerodynamic roughness of ice and snow on Round Lake is similar to that of open water, previously reported (Table 3).

[46] The data show that surface shear stress on the lake varies the most over the first 500 m downwind of the transition from the canopy along the shore onto the lake, and the shear stress at the transition point from the canopy to the lake surface extends to approximately zero. The canopy surrounding the lake was estimated in the field to be approximately 10 m high. The length of reduced shear stress therefore is found to be approximately $50h_c$ (Figure 11). This matches the results of the wind tunnel study and those by *Bradley and Mulhearn* [1983].

[47] Unlike a water surface, which deforms as the wind blows over it, a lake covered by ice with or without snow on it has properties analogous to a rigid flat plate. To determine whether the shear stress results from the data collected over the ice can be extended to open water conditions, shear stress on a flat plate for a distance of 1000 m, on the basis of the inversion of the friction law technique shown by *Schlichting and Gersten* [2000], and for open water were plotted as a function of wind speed (Figure 12). Shear stress at distance x = 1000 m is considered in this example to ensure that the turbulent boundary layer is fully developed and is comparable to the field scale. This is also the size of the lake in this experiment. The shear stress development over open water is calculated from equations (1)–(3). The result shows that the shear stress over a flat surface or ice-covered lake is comparable in magnitude to that on open water for a distance of 1000 m. In general, data collected over the ice are representative of open water conditions, although minor differences at small wind velocities (i.e., $U_{10} < 10$ m s^{-1}) are evident. Although wind speeds were not measured at a height of 10 m, it is safe to infer from the maximum wind velocity of 5 m s^{-1} measured at a height of 2.3 m that wind velocities at 10 m were less than the 10 m s^{-1} threshold.

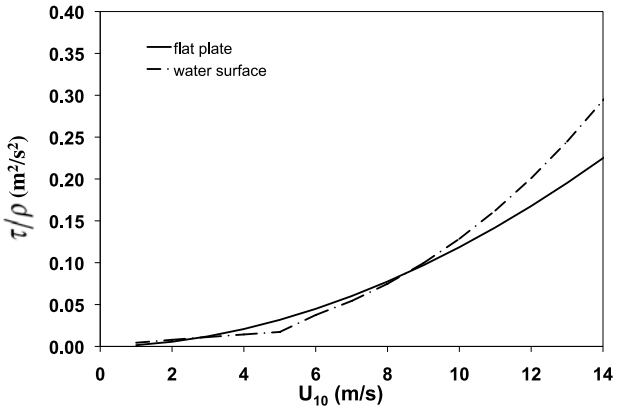

Figure 12. Plot of surface shear stress τ as a function of wind speed U over a flat plate (i.e., ice cover) at x = 1000 m and over a water surface (equation (1) with equations (3) and (4) for drag coefficients).

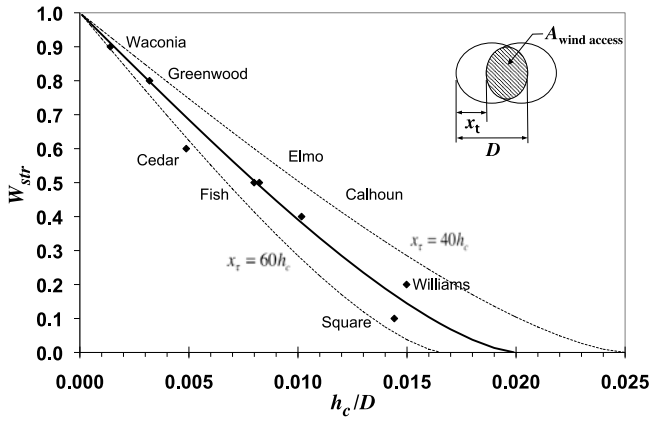

Figure 13. Wind-sheltering coefficient, W_{str}, as a function of canopy height, h_c, to lake diameter, D, ratio. The solid line gives the prediction by the wind-sheltered area model on the basis of wind tunnel and field experiments (equation (8)). Symbols are wind-sheltering coefficients from *Hondzo and Stefan* [1993] obtained by calibration of a one-dimensional water temperature stratification model for eight lakes of different sizes.

5.7. Application to Lake Modeling

[48] The theory for IBL development from a rough to a smooth surface suggests that a new equilibrium layer develops over the new surface without influence from the upwind surface. The experiments confirm this, and the extent of lake sheltering, in terms of a surface shear stress development downwind from a canopy, can be roughly related to canopy height. In terms of surface shear stress, wind sheltering is shown to extend over a length of approximately $40h_c$ to $60h_c$. Therefore, a lake with a diameter less then 40 to 60 times the adjacent canopy height (e.g., 10 to 15 m for mature forests and relatively dense-tree-lined shores) has a sheltered length of approximately 400 to 900 m. Such a lake will experience wind velocities and shear stresses significantly smaller than those measured, e.g., at a nearby airport or unsheltered station on or near a lake. The characteristic "shear deficit length" x_τ of $40h_c$ to $60h_c$ differs substantially from the reattachment length for the flow over a step, which is commonly given as $5h_c$ to $7h_c$ [*Aider et al.*, 2007].

[49] A simple geometrically based relationship to estimate the wind-sheltering coefficient for relatively round lakes based on the area of wind access can be derived using this shear deficit length with independent variables, lake size, and canopy height. The area of a lake where surface shear stress is not significantly reduced by wind sheltering approximates the area of wind access

$$A_{\text{wind access}} = \frac{D^2}{2}\cos^{-1}\left(\frac{x_\tau}{D}\right) - \frac{x_\tau}{2}\sqrt{D^2 - x_\tau^2}, \tag{7}$$

where D is the equivalent circular diameter of the lake, on the basis of lake surface area, A_{lake}. The wind-sheltering coefficient is then defined as the ratio of the area of wind access, equation (7), to the total lake surface area:

$$W_{\text{str}} = \frac{A_{\text{wind access}}}{A_{\text{lake}}} = \frac{2}{\pi}\cos^{-1}\left(\frac{x_\tau}{D}\right) - \left(\frac{2x_\tau}{\pi D^2}\right)\sqrt{D^2 - x_\tau^2}. \tag{8}$$

When the canopy height shrinks to zero, x_τ also diminishes and the area of wind access, as to be expected, approaches the total lake surface area. Similarly, a very large lake affectively has no wind sheltering, and the wind-sheltering coefficient equals 1.0.

[50] A range of predictions by equation (8) for $x_\tau/h_c = 40$, 50, and 60 are plotted along with calibration results from lake temperature model simulations (Figure 13). The new model for a priori estimation of the wind-sheltering coefficient is validated by comparison with calibrated wind-sheltering coefficient values W_{str}^+ from eight lakes of different sizes. The model-calibrated wind-sheltering coefficients are from *Hondzo and Stefan* [1993] that use wind data from nearby airports. The only data not previously recorded for these lakes were the average canopy heights surrounding the lakes. Topographic maps, satellite photos and field observations were used to estimate an appropriate canopy height for each of the lakes. Canopy heights ranged from 5 m for sparse shoreline trees and agricultural crops to 15 m for dense-old-growth forests with topographic relief.

[51] Determining an average canopy height is not trivial. One has to consider a number of factors such as the canopy coverage along the shore and the dominant direction of winds during the growing season. One should consider the tallest, most continuous canopy closest to the lake, because the influence of canopies further from the lake is decreased with distance and shorter canopies along the lake might be

Table 4. Summary of Wind-Sheltering Coefficients Predicted by the Wind-Sheltered Area Model for Eight Lakes Compared to Wind-Sheltering Coefficients Obtained by Calibration of a 1-D Water Temperature Stratification Model[a]

Lake	Surface Area (km^2)	Circular Diameter (km)	Calibrated Year	W_{str}^+	Near Lake Land Cover	h_c (m)	W_{str}
Thrush	0.07	0.30	1986	0.01	forest with relief	15	0.00
Williams	0.35	0.67	1984	0.2	forest/agricultural field	10	0.15
Square	0.85	1.04	1985	0.1	old-growth forest	15	0.17
Fish	1.16	1.22	1987	0.5	agricultural field/shoreline trees	10	0.49
Elmo	1.23	1.25	1988	0.5	agricultural field/shoreline trees	10	0.51
Calhoun	1.71	1.48	1971	0.4	suburban forest	15	0.38
Cedar	3.3	2.05	1984	0.6	agricultural field/shoreline trees	10	0.69
Greenwood	7.7	3.13	1986	0.8	forest/wetland	10	0.80
Waconia	10.0	3.57	1985	0.9	sparse shoreline trees	5	0.91

[a] W_{str}, wind-sheltering coefficients given by equation (8); W_{str}^+, calibrated wind-sheltering coefficients [*Hondzo and Stefan*, 1993]. Some characteristics of the eight lakes are also given.

sheltered by nearby larger ones. For example, if agricultural fields surround a lake, but a dense line (wind-break type) of trees border the shoreline, the canopy height should be considered as the wind-break height. Lake shape also affects the overall lake sheltering. Although a number of the lakes presented in Table 4 were not round and had variable canopy characteristics, considering an effectively round lake and constant canopy height for the wind sheltering estimate by equation (8) gave good results. The new wind-sheltering model shows good agreement with the 1-D model-calibrated wind-sheltering coefficients, and can be used to estimate wind-sheltering coefficients a priori.

[52] On the basis of the data set used to validate the new wind-sheltering model, it seems reasonable to expect that a well-defined (wind-break type) tree line along the lakeshore will produce an effect similar to a wide forest canopy in terms of downwind surface shear stress development. This can be seen in Figure 13 and Table 4 for Fish, Elmo, and Cedar lakes, which have a belt of trees along their shorelines. It would seem more important that the tree line be continuous and relatively dense. However, we did not investigate canopies of limited width in a rigorous way, and it would be premature to draw conclusions on a threshold density or width.

[53] Although this model was developed for nearly round lakes, the same geometric principle relating the shear deficit length and lake size is believed to apply to lakes of arbitrary shape. It is also important to note that the woody canopy elements along with foliage appear to be an important contributor to the sheltering effect. The field results, for a mostly deciduous canopy, show that even during the winter when there are no leaves, sheltering still occurs. This supports the importance of considering the roughness density or frontal area index as opposed to leaf area index when characterizing the canopy density as pointed out by *Raupach* [1994].

[54] While practical for 1-D lake models, the wind-sheltering coefficient discussed in section 5 neglects details of nonuniform wind speed distributions over lakes that are important for three-dimensional lake models [e.g., *Wang and Hutter*, 1998; *Wang et al.*, 2001; *Wang*, 2003; *Rueda et al.*, 2009]. Our results for surface shear stress development downwind of a canopy or a bluff may be useful as input to these modeling applications.

6. Conclusions

[55] Wind stress distribution on a lake surface is an important boundary condition for simulating lake circulation and water quality. However, the effect of vegetation canopies, buildings, and topography surrounding a lake on the distribution of surface shear stress on the lake is poorly understood. In this paper, the transition of the ABL wind field from a rough canopy or a bluff to a smooth surface and the associated surface shear stress (shear velocity) development have been explored experimentally.

[56] Experiments were conducted in a boundary layer wind tunnel to determine the extent of wind sheltering by a bluff or vegetation (tree) canopies of varying height, roughness, and porosity. Wind velocity profiles downwind from the canopies or bluff were measured, and shear stress distributions were derived from the measurements. Results of field experiments, conducted on the ice-covered Round Lake, validate the wind tunnel results. In both the wind tunnel and the field, a reduced surface shear stress over a distance of 40 to 60 times the canopy height was observed. These findings provide the basis for a simple but sufficiently accurate model to estimate wind-sheltering coefficients that can be used in numerical 1-D hydrodynamic/water quality models of stratified lakes. The new wind-sheltering model predicts a priori an area-based wind-sheltering coefficient on the basis of canopy height and lake size alone. Wind-sheltering coefficients predicted by the model were validated against those obtained by calibration of simulated lake temperature profiles for measurements in eight stratified lakes over a period of several years, and the a priori model results compare well to the a posteriori determined values (Figure 13). The results show that small lakes ($A_{\mathrm{Lake}} < 1\ \mathrm{km}^2$) will experience substantial sheltering if surrounded by a continuous canopy or a bluff greater than 10 m high.

[57] Another outcome of the study is the recognition that lake modelers should use wind velocity data collected near or on a lake cautiously. It is important to consider land cover near lakes when measuring wind speed on a lake for the purpose of lake processes simulation. It is likely that the wind data collected near or on a lake are not representative of the spatial distribution of wind over the lake surface. A better understanding of how wind sheltering impacts wind patterns on lakes, and how it affects the interpretation of measurements at a single point is required. The results from wind tunnel and field experiments provide useful information about how wind sheltering of a lake diminishes downwind of a canopy or a bluff. Wind direction is also important in interpreting wind data collected on or near a lake, especially for lakes of irregular shape or with heterogeneous land cover and topography. The model presented in this paper provides a tool to estimate the wind-sheltering coefficient of a (small) lake, which previously could not be determined without in situ measurements.

[58] **Acknowledgments.** This work was partially supported by NSF IGERT grant and the Department of Civil Engineering at the University of Minnesota. Support was provided for undergraduate researchers by the STC program of the National Science Foundation via the National Center for Earth-Surface Dynamics (grant EAR- 0120914). Experimental equipment was provided by the National Science Foundation (grant EAR-0537856) and NASA (grant NNG06GE256).

References

Aider, J. L., A. Danet, and M. Lesieur (2007), Large-eddy simulation applied to study the influence of upstream conditions on the time-dependent and averaged characteristics of a backward-facing step flow, *J. Turbul.*, *8*(51), 1–30.

Boehrer, B., and M. Schultze (2008), Stratification of lakes, *Rev. Geophys.*, *46*, RG2005, doi:10.1029/2006RG000210.

Bradley, E. F. (1968), A micrometeorological study of the velocity profiles and surface drag in the region modified by a change in surface roughness, *Q. J. R. Meteorol. Soc.*, *94*, 361–379, doi:10.1002/qj.49709440111.

Bradley, E. F., and P. J. Mulhearn (1983), Development of velocity and shear stress distributions in the wake of a porous shelter fence, *J. Wind Eng. Ind. Aerodyn.*, *15*, 145–156, doi:10.1016/0167-6105(83)90185-X.

Carper, M. A., and F. Porté-Agel (2008), Subfilter-scale fluxes over a surface roughness transition. part I: Measured fluxes and energy transfer rates, *Boundary Layer Meteorol.*, *126*, 157–179, doi:10.1007/s10546-007-9228-z.

Cassiani, M., G. G. Katul, and J. D. Albertson (2008), The effects of canopy leaf area index on airflow across forest edges: Large-eddy simulation and analytical results, *Boundary Layer Meteorol.*, *126*, 433–460, doi:10.1007/s10546-007-9242-1.

Chamorro, L., and F. Porté-Agel (2009), Velocity and surface shear stress distributions behind a rough-to-smooth surface transition: A simple new model, *Boundary Layer Meteorol.*, *130*, 29–41, doi:10.1007/s10546-008-9330-x.

Charnock, H. (1955), Wind stress on a water surface, *Q. J. R. Meteorol. Soc.*, *350*, 639–640, doi:10.1002/qj.49708135027.

Chen, J. M., T. A. Clack, M. D. Novak, and R. S. Adams (1995), A wind tunnel study of turbulent airflow in forest clear cuts, in *Wind and Trees*, edited by M. P. Coutts and J. Grace, pp. 71–87, Cambridge Univ. Press, New York.

Condie, S. A., and I. T. Webster (2001), Estimating stratification in shallow water bodies from mean meteorological conditions, *J. Hydraul. Eng.*, *127*(4), 286–292, doi:10.1061/(ASCE)0733-9429(2001)127:4(286).

Counihan, J., J. C. R. Hunt, and P. S. Jackson (1974), Wakes behind two-dimensional surface obstacles in turbulent boundary layers, *J. Fluid Mech.*, *64*(3), 529–563, doi:10.1017/S0022112074002539.

Davies-Colley, R. J. (1988), Mixing Depths in New Zealand Lakes, *N. Z. J. Mar. Freshwater Res.*, *22*, 517–527.

Detto, M., G. G. Katul, M. B. Siqueira, J.-Y. Juang, and P. Stoy (2008), The structure of turbulence near a tall forest edge: The backward-facing step flow analogy revisited, *Ecol. Appl.*, *18*(6), 1420–1435, doi:10.1890/06-0920.1.

Downing, J. A., et al. (2006), The global abundance and size distribution of lakes, ponds, and impoundments, *Limnol. Oceanogr.*, *51*(5), 2388–2397.

Farell, C., and A. K. S. Iyengar (1999), Experiments on the wind tunnel simulation of atmospheric boundary layers, *J. Wind Eng. Ind. Aerodyn.*, *79*, 11–35, doi:10.1016/S0167-6105(98)00117-2.

Finnigan, J. J. (2000), Turbulence in plant canopies, *Annu. Rev. Fluid Mech.*, *32*, 519–571, doi:10.1146/annurev.fluid.32.1.519.

Fischer, H. B., E. J. List, R. C. Y. Koh, J. Imberger, and N. H. Brooks (1979), Mixing in Inland and Coastal Waters, 483 pp., Academic, San Diego, Calif.

Flesch, T. K., and J. D. Wilson (1999), Wind and remnant tree sway in forest cutblocks. I. Measured winds in experimental cutblocks, *Agric. For. Meteorol.*, *93*, 229–242, doi:10.1016/S0168-1923(98)00112-9.

Ford, D. E., and H. G. Stefan (1980), Thermal predictions using an integral energy model, *J. Hydraul. Div. Am. Soc. Civ. Eng.*, *106*(1), 39–55.

Garratt, J. R. (1992), The Atmospheric Boundary Layer, 316 pp., Cambridge Univ. Press, New York.

Gorham, E., and F. M. Boyce (1989), Influence of lake surface area and depth upon thermal stratification and the depth of the summer thermocline, *J. Great Lakes Res.*, *15*(2), 233–245.

Hondzo, M., and H. G. Stefan (1993), Lake water temperature simulation model, *J. Hydraul. Eng.*, *119*(11), 1251–1273, doi:10.1061/(ASCE)0733-9429(1993)119:11(1251).

Hutchinson, G. E. (1957), *Geography, Physics and Chemistry*, vol. 1, 1015 pp., John Wiley, New York.

Irvine, M. R., B. A. Gardiner, and M. K. Hill (1997), The evolution of turbulence across a forest edge, *Boundary Layer Meteorol.*, *84*, 467–496, doi:10.1023/A:1000453031036.

Jaster, D. A., A. L. S. Perez, F. Porté-Agel, and H. G. Stefan (2007), Wind velocity profiles and shear stresses on a lake downwind from a canopy: Interpretation of three experiments in a wind tunnel, *Rep. 493*, St. Anthony Falls Lab., Univ. of Minn., Minneapolis.

Jovic, S., and M. Driver (1994), Backward-facing step measurements at low Reynolds number, Re_h = 5000, *NASA Tech. Memo., TM-108807*.

Le, H., P. Moin, and J. Kim (1997), Direct numerical simulation of turbulent flow over a backward-facing Step, *J. Fluid Mech.*, *330*, 349–374, doi:10.1017/S0022112096003941.

Liu, J., J. M. Chen, T. A. Black, and M. D. Novak (1996), E-ε modelling of turbulent air flow downwind of a model forest edge, *Boundary Layer Meteorol.*, *77*, 21–44, doi:10.1007/BF00121857.

Melville, W. K. (1996), The role of surface-wave breaking in air-sea interaction, *Annu. Rev. Fluid Mech.*, *28*, 279–321, doi:10.1146/annurev.fl.28.010196.001431.

Monismith, S. G., and S. MacIntyre (2009), The surface mixed layer in lakes and reservoirs, in *Encyclopedia of Inland Waters*, edited by G. E. Likens, pp. 568–582, Elsevier, Oxford, U. K.

Oke, T. R. (1987), *Boundary Layer Climates*, 2nd ed., 435 pp., Routledge-Taylor and Francis, New York.

Patton, E. G., R. H. Shaw, M. J. Judd, and M. R. Raupach (1998), Large-eddy simulation of windbreak flow, *Boundary Layer Meteorol.*, *87*, 275–306, doi: 10.1023/A:1000945626163.

Perez, A. L. S., D. A. Jaster, F. Porté-Agel, and H. G. Stefan (2007), Wind velocity profile and shear stresses downwind from a canopy: Experiments in a wind tunnel, *Rep. 492*, St. Anthony Falls Lab., Univ. of Minn., Minneapolis.

Raupach, M. R. (1994), Simplified expression for vegetation roughness length and zero-plane displacement as function of canopy height and area index, *Boundary Layer Meteorol.*, *71*, 211–216, doi:10.1007/BF00709229.

Rueda, F. J., and J. Vidal (2009), Currents in the upper mixed layer and in unstratified water bodies, in *Encyclopedia of Inland Waters*, edited by G. E. Likens, pp. 568–582, Elsevier, Oxford, U. K.

Rueda, F., J. Vidal, and G. Schladow (2009), Modeling the effect of size reduction on the stratification of a large wind-driven lake using an uncertainty-based approach, *Water Resour. Res.*, *45*, W03411, doi:10.1029/2008WR006988.

Schlichting, H., and K. Gersten (2000), *Boundary Layer Theory*, 8th ed., 799 pp., Springer, New York.

Stull, R. B. (1988), An Introduction to Boundary Layer Meteorology, 670 pp., Kluwer Acad., Norwell, Mass.

Thill, J. W. (2009), Wind velocity measurements on two small ice covered lakes: A compilation of data with some results and discussion, *Rep. 527*, St. Anthony Falls Lab., Univ. of Minn., Minneapolis.

Vickers, D., and L. Mahrt (1997), Fetch limited drag coefficients, *Boundary Layer Meteorol.*, *85*, 53–79, doi:10.1023/A:1000472623187.

Walker, I. J., and W. G. Nickling (2003), Simulation and measurement of surface shear stress over isolated and closely spaced transverse dunes in a wind tunnel, *Earth Surf. Processes Landforms*, *28*, 1111–1124, doi:10.1002/esp.520.

Wang, Y. (2003), Importance of subgrid-scale parameterization in numerical simulations of lake circulation, *Adv. Water Resour.*, *26*, 277–294, doi:10.1016/S0309-1708(02)00166-5.

Wang, Y., and K. Hutter (1998), A semi-implicit semispectral primitive equation model for lake circulation dynamics and its stability performance, *J. Comput. Phys.*, *139*, 209–241, doi:10.1006/jcph.1997.5850.

Wang, Y., K. Hutter, and E. Bäuerle (2001), Three-dimensional wind-induced baroclinic circulation in rectangular basins, *Adv. Water Resour.*, *24*, 11–27, doi:10.1016/S0309-1708(00)00034-8.

Wanninkhof, R., J. Ledwell, and W. S. Broecker (1985), Gas exchange-wind speed relation measured with sulfur hexafluoride on a lake, *Science*, *227*, 1224–1226, doi:10.1126/science.227.4691.1224.

Wanninkhof, R., J. Ledwell, and J. Crusius (1990), Gas transfer velocities on lakes measured with sulfur hexafluoride, in *Air Water Mass Transfer: Selected Papers From the Second International Symposium on Gas Transfer at Water Surfaces*, edited by S. C. Wilhelms and J. S. Gulliver, 795 pp., Am. Soc. of Civ. Eng., Reston, Va.

Wanninkhof, R., W. E. Asher, D. T. Ho, C. Sweeney, and W. R. McGillis (2009), Advances in quantifying air-sea gas exchange and environmental forcing, *Annu. Rev. Mater. Sci.*, *1*, 213–244, doi:10.1146/annurev.marine.010908.163742.

Wilson, J. D., and T. K. Flesch (1999), Wind and remnant tree sway in forest cutblocks. III. A windflow model to diagnose spatial variation, *Agric. Meteorol.*, *93*, 259–282, doi:10.1016/S0168-1923(98)00121-X.

Wüest, A., and A. Lorke (2003), Small-scale hydrodynamics in lakes, *Annu. Rev. Fluid Mech.*, *35*, 373–412, doi:10.1146/annurev.fluid.35.101101.161220.

Yang, B., M. R. Raupach, R. H. Shaw, K. T. Paw U, and A. Morse (2006), Large-eddy simulation of turbulent flow across a forest edge. Part I: Flow statistics, *Boundary Layer Meteorol.*, *120*, 377–412, doi:10.1007/s10546-006-9057-5.

D. A. Jaster, C. D. Markfort, F. Porté-Agel, H. G. Stefan, and J. W. Thill, Saint Anthony Falls Laboratory, University of Minnesota–Twin Cities, Minneapolis, MN 55414, USA. (mark0340@umn.edu)

A. L. S. Perez, National Center for Earth-Surface Dynamics, University of Minnesota–Twin Cities, Minneapolis, MN 55414, USA.